INSTITUTE FOR FUSION STUDIES

DE-FG03-96ER-54346-789 IFSR #789

Space Charge Tracking Code for a Synchrotron Accelerator

M.B. OTTINGER AND T. TAJIMA
Institute for Fusion Studies
and Department of Physics
The University of Texas at Austin
Austin, TX 78712

June 1997

THE UNIVERSITY OF TEXAS

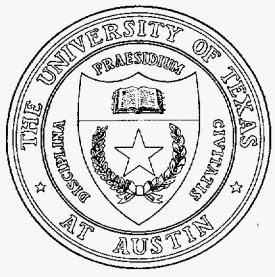

AUSTIN

Space Charge Tracking Code for a Synchrotron Accelerator

M.B. Ottinger and T. Tajima
Department of Physics and Institute for Fusion Studies
The University of Texas at Austin
Austin, Texas 78712 USA
and
K. Hiramoto
Hitachi Research Lab.
Hitachi Ltd. Hitachi-shi
Ibaraki-ken, 316, Japan

May 30, 1997

Abstract

An algorithm has been developed to compute particle tracking, including self-consistent space charge effects for synchrotron accelerators. In low-energy synchrotrons space charge plays a central role in enhancing emittance of the beam. The space charge effects are modeled by mutually interacting (through the Coulombic force) N cylindrical particles (2-$\frac{1}{2}$-dimensional dynamics) whose axis is in the direction of the equilibrium particle flow. On the other hand, their interaction with synchrotron lattice magnets is treated with the thin-lens approximation and in a fully 3-dimensional way. Since the existing method to treat space charge fully self-consistently involves 3-D space charge effect computation, the present method allows far more realistic physical parameters and runs in far shorter time (about 1/20). Some examples on space charge induced instabilities are presented.

DISCLAIMER

1 Introduction

The synchrotron is the latest circular accelerator in a long evolution of particle accelerators. It consists of modular units of magnets which can be flexibly designed and modified and has superior beam optical properties because of various higher-order multipoles at our discretion.

For these reasons many (or most) of high energy accelerators of nonradiative particles, as well as many lower energy accelerators of late, are synchrotrons. The latter includes examples of low-energy injectors/boosters to high energy synchrotrons and medical synchrotrons.

There are many subtle effects and instabilities that can affect the performance of high energy synchrotrons (see surveys in [1], [2], [3]), some of which arise due to the higher-order nonlinearities of magnets and their cumulative effects. On the other hand, lower energy counterparts tend to have less elements (such as magnets) and may suffer from less subtle higher-order resonances, while they suffer more from space charge effects. This is because the space charge electric field, E_r, due to the beam charges , is partially compensated by the current carried by the beam as $E_r - v_z B_\theta / c \approx 1/\gamma^2 E_r$, where γ is the relativistic factor. Because of the space charge effect's strong γ-dependence, it can heavily influence nonrelativistic portions of the synchrotron operation. The best known detrimental effect is the emittance degradation (the emittance is a quantity that measures the phase space volume of the beam). Because of this emittance degradation, when we try to increase the current (and thus the amount of space charge) in the low-energy synchrotron, the space charge effect either degrades the beam badly or even disrupts it, leading to the threshold current above which the synchrotron does not operate. It is thus very important to understand the process of this emittance degradation. However, because of its collective nature and highly nonlinear physics, it is not well understood.

To gain more understanding, it is necessary to develop a fully self-consistent numerical

simulation code that is both accurate within an affordable computational resource and sufficiently flexible to probe physical parameter dependences and the mechanism for this process. In a synchrotron the design (i.e. desired equilibrium) orbit is a perfect coasting curve (such as a circle, if the machine is circular). Particles that are slightly away from the design orbit will oscillate around this orbit (called the betatron orbit) due to the restoring magnetic field of the synchrotron magnets (often called the "lattice" of magnets). The oscillation frequency is referred to as the tune (ν).

An example of problems we are interested in is the phenomenon of resonance of particle dynamics between the betatron oscillation and the "external" (i.e. other forces, such as space charge noise) drivers. When the beam tune is equal to a half-integer (0.5, 1.0, 1.5, etc.) a resonance can be created between the betatron oscillation and an error (non-designed field) in the magnetic structure. This is similar to a harmonic oscillator in resonance with a small driving force causing in increase in the oscillator amplitude. Traditionally, this effect was believed to occur exactly at the half-integer tune, but further theoretical work published by Richard Baartman suggests that the resonance should occur at a point slightly below the half-integer [4].

There are two principal groups of forces that can govern the particle trajectories: the external, or machine-induced forces and the internal, or space charge forces. The first, and stronger set, is from the electric and magnetic fields created by the synchrotron elements which accelerate the beam (RF cavities), bend the beam (dipole magnets), and focus the beam (quadrupole magnets). The fields are determined by the machine design and are independent of the beam characteristics. When these are the only forces acting on the beam particles, an analytic solution to the beam's progression can be obtained. This solution would include the beam tune and the time evolution of the beam emittance.

The second set of forces which may act on the beam particles is the electric and magnetic interaction forces between the beam particles, or space charge force. This force is dynamic

in nature, as it is determined by the relative positioning of the beam particles while they move through the lattice. As this force becomes important in the particle trajectory, it is no longer possible to obtain a simple analytical solution for the beam evolution. Even an approximate solution for the beam envelope equation is complex [5]. For this reason it is necessary to study the beam evolution through numerical simulation.

The traditional method of beam tracking is to approximate the beam with a set of non-interacting macro-particles occupying the six-dimensional beam phase space. As the macro-particles advance through the elements in the synchrotron lattice, appropriate momentum kicks are applied [6]. For models where space charge is important, at given time intervals the space charge fields are determined with a three-dimensional PIC (Particle in Cell) algorithm. These fields are then used to calculate the momentum change of each particle [7].

Memory and time constraints introduce two related, drawbacks to this method. The first is the limitation on the number of macro-particles. However, for the dynamics of the charged particles in a synchrotron to be essentially collisionless, the plasma parameter, g, must be much less than unity. The plasma parameter is given by $g = (n\lambda_D^3)^{-1}$ where n is the particle density and $\lambda_D = (T_i/4\pi n_i e^2)^{1/2}$ with T_i as the temperature around the equilibrium momentum. In a coarse 3-D simulation (e.g. using around 1000 macro-particles) this number becomes larger than unity, while it is much smaller than unity in a realistic machine. The second problem is the computational time restraint on the number of grids allowed in the space charge calculation. In a PIC simulation [8], the space charge force is obtained by solving Poisson's equation with a Fast Fourier Transform (FFT) on a three-dimensional grid. The computation time required to perform the FFT is proportional to $M^d \ln M^d$ where M is the typical number of grids and d is the number of spatial dimensions. Since most of the simulation run time is used in the FFT, the number of grids is severely limited in a 3-D simulation.

To study the instabilities in the low-energy synchrotron through numerical simulation,

we needed to develop a simulation model which would accurately track the particles through the synchrotron lattice, include the space charge perturbations, and run at a fast enough rate to be computationally reasonable. We have developed such a model and have encoded it into program SYN2D. This paper presents our model and its region of validity, describes our code, and demonstrates through a comparison of data from theory, a previous tracking model, and SYN2D that our model provides reasonable outcome.

2 Description of Model

We consider a positively-charged ion beam propagating through a synchrotron accelerator. The beam coordinates are aligned with the x-coordinate as the direction of beam propagation, the x-coordinate as the outward horizontal direction (orbital bends are in the negative x-direction), and the y-coordinate as the vertical direction. Its transverse size, σ_x and σ_y, is much smaller than its longitudinal length S (i.e. it is cigar shaped) and is much smaller than the synchrotron's radius of curvature. With these requirements at any position in the synchrotron, for the purpose of calculating space charge effects, the beam can be approximated as an infinitely long, straight, uniform beam. Space charge of the beam is then independent of the s-coordinate and may be calculated in 2-$\frac{1}{2}$-dimensions, similar to the case examined by Chen, *et al.* [9].

Our model approximates the beam as a set of N_p cylindrical macro-particles of finite radius, a_x and a_y (where $a_x \ll \sigma_x$ and $a_y \ll \sigma_y$). The macro-particles are aligned parallel to the s-axis, with a length which is long compared to the beam radius, such that they can be considered infinitely long in the space charge calculation, yet shorter than the synchrotron dimensions, such that they can pass quickly through the synchrotron elements. Each macro-particle has a dimensionless velocity $(\beta_x, \beta_y, \beta_s)$, transverse position (x, y), and longitudinal reference point (s) with respect to the lattice of magnets.

2.1 Dimensionless Equation of Motion

Since the two sets of forces that act upon the macro-particles (external synchrotron magnetic and electric and the internal space charge) are electromagnetic in nature, the equation of motion can be obtained from the Lorentz force equation:

$$\frac{d\mathbf{P}}{dt} = e[\mathbf{E} + \boldsymbol{\beta} \times \mathbf{B}], \tag{1}$$

where $\mathbf{P}$ is the macro-particle's momentum, e is the macro-particle's charge, and $\mathbf{E}$ and $\mathbf{B}$ are the transverse electric and magnetic fields at the macro-particle.

To remove the dimensionality of Eq. (1) we introduce the following dimensionless parameters for time, electric field, and magnetic field:

$$\tau = \omega_p t, \tag{2}$$

$$\boldsymbol{\xi} = \frac{e\mathbf{E}}{\omega_p mc}, \tag{3}$$

$$\boldsymbol{\zeta} = \frac{e\mathbf{B}}{\omega_p mc}, \tag{4}$$

where m is the macro-particle's rest mass, and ω_p is a reference plasma frequency. Replacing the momentum $\mathbf{P}$ by its constituent factors of mass, relativistic Lorentz factor, and velocity ($\mathbf{P} = m\gamma\boldsymbol{\beta}c$), we can rewrite Eq. (1) in dimensionless form

$$\frac{d\gamma\boldsymbol{\beta}}{d\tau} = \boldsymbol{\xi} + \boldsymbol{\beta} \times \boldsymbol{\zeta}. \tag{5}$$

The electric and magnetic fields can be split into two parts: the synchrotron component, and the space charge component,

$$\xi = \xi_{\text{syn}} + \xi_{\text{spc}}, \tag{6}$$

$$\zeta = \zeta_{\text{syn}} + \zeta_{\text{spc}}. \tag{7}$$

The macro-particles feel a continuous radial force from the space charge. However, the components from the synchrotron elements are zero, except when the particle's reference point passes through an element. Because of this, the macro-particle's equation of motion can be divided into two regions: with and without external fields. In the next subsection we solve the equation of motion as the macro-particle passes through the element and in the following we solve for the equation of motion in the drift regions.

2.2 Equation of Motion With Non-zero External Field

The synchrotron elements can be treated as thin elements [6]. Then we take the time to pass through one much smaller than the timestep used in the space charge calculation. These "kicks" can then be treated as impulses, changing the instantaneous velocity, but not the instantaneous position. This technique has been developed by Schachinger and Talman and used in their code TEAPOT [6].

Synchrotron elements include two types: RF cavities, which have a longitudinal electric field and no magnetic field, and magnetic multipole elements, in which the electric field is zero.

The macro-particle's equation of motion as it passes through an RF cavity is given by:

$$\frac{d\gamma\beta_x}{d\tau} = 0, \tag{8}$$

$$\frac{d\gamma\beta_y}{d\tau} = 0, \tag{9}$$

$$\frac{d\gamma\beta_s}{d\tau} = \xi_s. \tag{10}$$

Finite differencing these equations to first order in β_x/β_s, β_y/β_s, and $\xi_s d\tau/\beta_s$ yields

$$\beta_x^+ = \beta_x^-, \tag{11}$$

$$\beta_y^+ = \beta_y^-, \tag{12}$$

$$\beta_s^+ = \beta_s^- + \frac{1}{\gamma^-}\xi_s d\tau, \tag{13}$$

where the "+" denotes the quantity just after the element and the "−" just before the element.

The equation of motion as the macro-particle passes through a magnetic element is given as

$$\frac{d\gamma\boldsymbol{\beta}}{d\tau} = \boldsymbol{\beta} \times \boldsymbol{\zeta}, \tag{14}$$

where the magnetic field $\boldsymbol{\zeta}$ is calculated from its multipole components as

$$\zeta_x + i\zeta_y = \sum_{n=0}^{n_{\text{poles}}} (b_n + ia_n)(x_i + iy_i)^n, \tag{15}$$

with a_n and b_n as the n^{th} skew and straight multipole factors of the lattice element. Finite differencing the equation of motion with $d\tau$ equal to the time spent inside the lattice ($d\tau = \gamma\beta_s/1+\delta$ where $1+\delta$ is the fractional difference between the macro-beam's momentum and the beam's design momentum) and solving for the particle velocities after the magnet, we get

$$\beta_x^+ = \beta_x^- - \frac{\beta_s}{1+\delta}\zeta_y, \tag{16}$$

$$\beta_y^+ = \beta_y^- + \frac{\beta_s}{1+\delta}\zeta_x, \tag{17}$$

$$\beta_s^+ = \sqrt{(\beta_s^-)^2 + (\beta_x^-)^2 + (\beta_y^-)^2 - (\beta_x^+)^2 - (\beta_y^+)^2}. \tag{18}$$

ζ_x and ζ_y are obtained from Eq. (15). The longitudinal velocity change, Eq. (18), is obtained from the identity that a magnet does not alter the particle energy (i.e. γ is constant). The code SYN2D applies these velocity shifts, Eqs. (13) and (16)–(18), to the macro-particles as their reference points pass through the elements. The exact method is described later.

2.3 Equation of Motion Without External Fields

While the macro-particles pass between the magnetic elements (an area known as the drift region which makes up a vast majority of the synchrotron ring) the electric and magnetic fields in Eq. (5) have only a space charge component. Since the space charge electric and magnetic fields are related as $\boldsymbol{\zeta} = \boldsymbol{\beta} \times \boldsymbol{\xi}$, Eq. (5) can be rewritten as

$$\frac{d\boldsymbol{\beta}\gamma}{d\tau} = \boldsymbol{\xi}(1-\beta^2) + (\boldsymbol{\beta}\cdot\boldsymbol{\xi})\boldsymbol{\beta}. \tag{19}$$

By extracting the factor γ from the derivative and evaluating Eq. (19) to first order in β_x/β_s and β_y/β_s and with $\xi_s = 0$, the components for the equations of motion become:

$$\frac{d\beta_x}{d\tau} = \xi_x\gamma^{-3}, \tag{20}$$

$$\frac{d\beta_y}{d\tau} = \xi_y\gamma^{-3}, \tag{21}$$

$$\frac{d\beta_s}{d\tau} = \beta_s\gamma^{-3}(\beta_x\xi_x + \beta_y\xi_y). \tag{22}$$

When finite differenced, Eqs. (20)–(22) become

$$\beta_x^{n+1} = \beta_x^n + \Delta\tau\xi_x\gamma^{-3}, \tag{23}$$

$$\beta_y^{n+1} = \beta_y^n + \Delta\tau\xi_x\gamma^{-3}, \tag{24}$$

$$\beta_s^{n+1} = \beta_s^n + \Delta\tau\beta_s^n\gamma^{-3}\left[\beta_x^n\xi_x + \beta_y^N\xi_y\right]. \tag{25}$$

3 Particle Tracking Code SYN2D

We have developed a tracking code, titled SYN2D, for tracking the macro-particles around a synchrotron accelerator ring, using our 2-$\frac{1}{2}$-dimensional model for the space charge calculations. SYN2D uses two main input files. The first, giving the lattice characteristics, is obtained from an output file produced by Talman and Schachinger's tracking code TEAPOT [6],

which reads in a standard synchrotron lattice file and converts it into a thin element lattice file containing the magnitudes and positions of each thin lattice element. The second input file is defined by the user and lists the simulation parameters (timestep, particle number, number of turns, etc.) and the beam characteristics (emittances, current, initial distribution, etc).

The code, SYN2D, reads in the two input files, creates the initial particle distribution, tracks the particles (as outlined below), and records the desired diagnostics (currently, the beam emittance and tune-shift at the end of each turn).

The particle tracking is accomplished using Eqs. (13), (16)–(18), and (23)–(25). First, each of the particles is advanced in space according to

$$\widehat{x}_i^{n+1} = \widehat{x}_i^n + \beta_x^n \widehat{c} \Delta\tau, \tag{26}$$

$$\widehat{y}_i^{n+1} = \widehat{y}_i^n + \beta_y^n \widehat{c} \Delta\tau, \tag{27}$$

$$\widehat{s}_i^{n+1} = \widehat{s}_i^n + \beta_s^n \widehat{c} \Delta\tau, \tag{28}$$

where the hats denote the dimensionless quantities:

$$\widehat{x} = \frac{x}{x_g}, \tag{29}$$

$$\widehat{y} = \frac{y}{x_g}, \tag{30}$$

$$\widehat{s} = \frac{s}{x_g}, \tag{31}$$

$$\widehat{c} = \frac{c}{\omega_p x_g}, \tag{32}$$

and x_g is the simulation gridsize. For convenience we will no longer explicitly write the hat, but they will be implied.

If the macro-particle passes through a lattice element during this timestep, the beam is advanced in space using Eqs. (26)–(28) with $\Delta\tau$ replaced by $\Delta\tau_e$, which is the time for the

particle to reach the element. The velocities are then shifted, using Eqs. (13) or (16)–(18), and the beam is advanced again using the remainder of the timestep ($\Delta\tau - \Delta\tau_e$). At the end of the timestep the electric fields are calculated from Poisson's equation with an FFT algorithm. The electric fields are used in Eqs. (23)–(25) to give the new macro-particle velocities. This process then repeats for the next timestep.

At the end of each complete cycle around the lattice the macro-particle's phase space positions are recorded and used to calculate the fractional part of the tune and the beam emittance.

4 Testing of the Code

We define the operating regimes of the code and test the code against the theoretical and other computational results. In selecting the simulation parameters of macro-particle number and timestep we needed to select values that were sufficient enough not to affect the data, yet not overpowering to make the code inefficient. It was decided to perform several test runs using a current of 1.0 amps (which is relatively large for this code) and observe the impact of varying the macro-particle number and timestep for runs of 25 turns. We then used the optimal parameters and compared run times with the 3-D code. The results are given below.

4.1 Regimes of Simulation Parameters

To measure the effect of the number of macro-particles on the beam tune and emittance, a series of simulations were performed with a current of 1.00 Amps, energy of 10 MeV, horizontal emittance of 50 π mm-mrad, vertical emittance of 10 π mm-mrad, and timestep of 0.2. Each simulation had a different number of macro-particles ranging from 16 to 4096. Figure 1-a shows the average vertical tune-shifts and relative vertical emittances (average rms emittance divided by initial rms emittance) over each 25 turn run with error bars giving

the rms fluctuation of these values. The horizontal tune-shifts and relative emittances are sufficiently similar to their vertical counter parts that only the vertical ones are shown. As can be seen, in simulations with 512 macro-particles or more, the tune-shifts remain constant with only small fluctuation and the relative emittance is also constant with only slight fluctuations. To keep the simulation time efficient and without major variations in emittance or tune-shifts, we have opted to use 1028 macro-particles in most simulation runs.

The next important parameter we tested was timestep ($\Delta\tau$). Since the simulation run time is inversely proportional to the timestep we need to make $\Delta\tau$ as large as possible. However, in the derivation of the equations of motion we used the approximation that $\Delta\tau$ was sufficiently less than 1.0. To determine the optimal timestep, we performed several simulation runs while varying the timestep from 0.05 to 1.6. In each of these runs we used a current of 1.00 amps, energy of 10 MeV, horizontal emittance of 50 π mm-mrad, vertical emittance of 10 π mm-mrad, and 1024 macro-particles. The resulting vertical tune-shifts and relative vertical emittances are shown in Fig. 1-b. The horizontal and vertical data produced similar results so we only present the vertical data. As can be seen, for timesteps less than or equal to 0.8 the tune-shifts remain fairly constant with only small fluctuations, as they should. For timesteps less than 0.4 the relative vertical emittance remains constant, as expected, with little variance. We have chosen to run our code using a timestep of 0.2.

The table below lists several of the simulation parameters for a typical run on our code. The column on the left gives the dimensionless parameters, with N_τ being the number of timesteps per complete turn. The column on the right has the parameters in SI units.

CODE PARAMETERS	
Parameters for a typical run: $I = 1.0$ amps, $E = 10$ MeV, $\epsilon_x = 50\pi$ mm-mrad, $\epsilon_y = 10\pi$ mm-mrad, $N_p = 1024$, $d\tau = 0.2$	
Dimensionless Parameters	Parameters in SI Units
$\widehat{c} = 1120$ $a_x = 0.5$ $a_y = 0.5$ $\sigma_x = 4.7$ $\sigma_y = 2.1$ $N_\tau = 52.4$	$x_g = 0.0189$ m $\omega_p = 1.42 \times 10^7$ Hz $d\tau = 1.41 \times 10^{-8}$ s $\lambda = 2.25 \times 10^{-11}$ C/m

We performed runs with the same parameters on our SYN2D and SIMPSONS [7] (a 3-D PIC code for synchrotron space charge calculations) to compare run times. In both cases, identical lattices and beam parameters were used and both were run on the same CRAY-2 machine. The code SIMPSONS completed tracking 1024 particles for 100 turns in 2350 CPU seconds. SYN2D completed the simulation in 105 CPU seconds. This is an improvement by more than a factor of 20. Our code, therefore, makes more simulation runs and longer runs possible.

4.2 Comparison of Theory and Simulation

In this section we compare the tune-shifts obtained from our code with those from a theoretical equation, and with those obtained from the 3-D code SIMPSONS. We first show the derivation of the theoretical equation. Then we present graphically a comparison between that equation and the simulations for varying current, energy and emittances.

4.2.1 Theoretical equation

The theoretical equation we employ is a modification of the Laslett tune shift formula [10, 11] which gives the tune shift as a function of beam energy, emittance and intensity. To derive this equation, we consider a beam of constant, uniform density with an elliptical transverse

cross-section such that the beam surface can be written as

$$\frac{x^2}{a^2} + \frac{y^2}{b^2} = 1. \tag{33}$$

Or, in other words, a beam with density

$$n(x,y,s) = \begin{cases} n_o \text{ for } & \frac{x^2}{a^2} + \frac{y^2}{b^2} \leq 1, \\ 0 \quad \text{for} & \frac{x^2}{a^2} + \frac{y^2}{b^2} > 1. \end{cases} \tag{34}$$

We require that the transverse beam size (a, b) be much smaller than the synchrotron circumference such that the beam can be approximated as an infinitely long straight beam (para-axial approximation). We also require that the longitudinal velocity (β_s) be much greater than the tra verse velocities (β_x, β_y).

To obtain the spa harge effect, we use the density of Eq. (34) to solve Poisson's equation $(\nabla^2 \Phi_o = -en_o/\epsilon_o i)$ for the scalar electric potential Φ_o. The solution for $x^2/a^2 + y^2/b^2 < 1$ is [5]

$$\Phi_o(x,y) = -\frac{en_o}{2\epsilon_o}\left[\frac{bx^2}{a+b} + \frac{ay^2}{a+b}\right]. \tag{35}$$

Inside the beam the electric field is given by the gradient of the scalar potential

$$\mathbf{E}(x,y) = -\nabla\Phi_o = \frac{en_o}{\epsilon_o(a+b)}(bx\hat{e}_x + ay\hat{e}_y), \tag{36}$$

and the internal magnetic field is given by the cross product of the beam velocity and the electric field

$$\mathbf{B}(x,y) = \frac{1}{c}\boldsymbol{\beta} \times \mathbf{E} \approx \frac{en_o\beta_s}{\epsilon_o(a+b)c}(-ay\hat{e}_x + bx\hat{e}_y). \tag{37}$$

Using Eqs. (36) and (37), we get the space charge force as

$$\mathbf{F}_{sp} = \frac{e^2 n_o}{\epsilon_o(a+b)}\left[(1-\beta_s^2)bx\hat{e}_x + (1-\beta_s^2)ay\hat{e}_y\right] = \frac{e^2 n_o}{\epsilon_o(a+b)\gamma^2}\left[bx\hat{e}_x + ay\hat{e}_y\right]. \tag{38}$$

The space charge effect on the transverse particle dynamics in the presence of the lattice magnets is now expressed in the following form. With the force from the quadrupole magnetic

field of the synchrotron

$$\mathbf{F}_{\text{syn}} = -m\gamma c^2 \beta_s^2 (\kappa_{x,\text{syn}}(s) x \hat{e}_x + \kappa_{y,\text{syn}}(s) y \hat{e}_y), \tag{39}$$

where $\kappa_{\text{syn}}(s)$ is the quadrupole magnetic moment at the position s, the combined space charge force and quadrupole force give rise to the equation of motion as

$$\frac{d^2x}{ds^2} = \left[\frac{e^2 n_o b}{\epsilon_o (a+b) \gamma^3 m c^2 \beta_s^2} - \kappa_{x,\text{syn}}(s) \right] x = \left[\kappa_{x,\text{spc}} - \kappa_{x,\text{syn}}(s) \right] x, \tag{40}$$

$$\frac{d^2y}{ds^2} = \left[\frac{e^2 n_o a}{\epsilon_o (a+b) \gamma^3 m c^2 \beta_s^2} - \kappa_{y,\text{syn}}(s) \right] y = \left[\kappa_{y,\text{spc}} - \kappa_{y,\text{syn}}(s) \right] y. \tag{41}$$

The total tune $\nu_{x,y}$ is defined as the number of transverse (x or y direction) oscillations the beam particles make as they complete one longitudinal revolution

$$\nu_{x,y} = -\frac{1}{4\pi} \int_S \beta_{cs}^{x,y} \kappa_{x,y}(s) ds, \tag{42}$$

where $\kappa_{x,y}(s)$ is the quantity in brackets in Eqs. (40) and (41) and $\beta_{cs}^{x,y}$ is the Courant-Snyder beta function [12] and is determined by the accelerator lattice design (i.e. it is independent of the beam parameters).

Since, in this approximation, $\kappa_{(x,y),\text{syn}}$ and $\kappa_{(x,y),\text{spc}}$ are independent of each other, the equation for the tune can be broken down into two parts: 1) the tune without space charge, $\nu_{(x,y)o}$, and 2) the tune-shift due to the space charge $\Delta\nu_{(x,y)} = \nu_{(x,y)} - \nu_{(x,y)o}$. The total tune is

$$\nu_x = \nu_{x,o} - \frac{e^2}{4\pi\epsilon_o \gamma^3 m c^2 \beta_s^2} \int_S \beta_{cs}^x \frac{b n_o}{a+b} ds, \tag{43}$$

$$\nu_y = \nu_{y,o} - \frac{e^2}{4\pi\epsilon_o \gamma^3 m c^2 \beta_s^2} \int_S \beta_{cs}^y \frac{a n_o}{a+b} ds. \tag{44}$$

Assuming that the values of a, b, n_o, and β_{cs} vary only slightly from their average values, the integrals can be approximated to give

$$\nu_x = \nu_{x,o} - \frac{e^2}{4\pi\epsilon_o \gamma^3 m c^2 \beta_s^2} S \overline{\beta}_{cs}^x \frac{\overline{b}\overline{n}_o}{\overline{a}+\overline{b}}, \tag{45}$$

$$\nu_y = \nu_{y,o} - \frac{e^2}{4\pi\epsilon_o\gamma^3 mc^2\beta^2} S\bar{\beta}^y_{cs}\frac{\overline{an}_o}{\bar{a}+\bar{b}}. \tag{46}$$

Defining the beam current (I) and beam RMS emittances ($\epsilon_{x,y}$) as

$$I = e\overline{n}_o\beta_s c\pi\bar{a}\bar{b}, \tag{47}$$

$$\epsilon_x = \frac{\gamma\beta\bar{b}^2}{4\beta_{cs,x}}, \tag{48}$$

$$\epsilon_y = \frac{\gamma\beta\bar{a}^2}{4\beta_{cs,y}}, \tag{49}$$

the tune-shifts can be obtained from Eqs. (45) and (46) as

$$\Delta\nu_x = \nu_x - \nu_{x,o} = \frac{-ISe}{16\pi^2\epsilon_o mc^3\beta^2\gamma^2\epsilon_x\left(1+\sqrt{\frac{\epsilon_y}{\epsilon_x}}\right)}, \tag{50}$$

$$\Delta\nu_y = \nu_y - \nu_{y,o} = \frac{-ISe}{16\pi^2\epsilon_o mc^3\beta^2\gamma^2\epsilon_y\left(1+\sqrt{\frac{\epsilon_x}{\epsilon_y}}\right)}. \tag{51}$$

The tune-shift is one of the most important parameters to characterize the effect of space charge. In general the larger the space charge (and thus the current), the greater the tune-shift (in the negative direction) is.

4.2.2 Comparison with Simulation

We performed four groups of simulation runs on SYN2D and SIMPSONS to see how the tune-shift depended upon the beam parameters (current, energy, horizontal emittance, and vertical emittance). In the first set of runs we varied the current from 0.0 to 2.0 amps while holding all other parameters constant. During these runs the energy was set to 10.0 MeV, and the horizontal and vertical emittances were set to 50 π mm-mrad and 10 π mm-mrad respectively. Each run lasted for 25 turns. At each turn the beam's horizontal and vertical tune-shifts were calculated and at the end of each run and the average tune-shift was recorded as well as the rms fluctuation in tune-shift over the run. Figure 2-a shows the average horizontal beam

tune-shifts as a function of current. The solid line on each graph represents the theoretical tune-shift obtained from Eqs. (50) and (51). The diamond point is the average tune-shift from our code and the horizontal dash is the average tune-shift from the code SIMPSONS. The error bars represent the rms fluctuation in tune-shift. Only horizontal tune-shifts are presented as the horizontal and vertical data show similar agreements.

Next we compared the tune-shifts while varying the beam energy. During these runs the current was set to 0.1 amps and the emittances were set to 50 π mm-mrad for the horizontal emittance and 10 π mm-mrad for the vertical emittance. The energy was varied between 1 MeV and 20 MeV. The runs went for 25 turns and the same technique was employed for obtaining the average beam tune-shifts. Figure 2-b shows the comparison between the theory, SYN2D, and SIMPSONS.

Finally, we tested the effect of the beam emittances on the tune-shift. This was done in two sets of runs. In both sets the current was fixed at 0.1 amps and the energy was set to 10 MeV. In the first set the vertical emittance was set to 10 π mm-mrad and the horizontal emittance was varied between 10 π mm-mrad and 50 π mm-mrad. The resulting tune-shifts are shown in Fig. 2-c. For the second set of runs the horizontal emittance was set at 10π mm-mrad and the vertical emittance was varied between 10 π mm-mrad and 50 π mm-mrad. The resulting tune-shifts are shown in Fig. 2-d.

Each of these figures have shown a good agreement between the theoretical tune-shift and our code. The figures have also shown that the tune-shifts are comparable with those obtained using the slower code SIMPSONS.

5 Application to Synchrotron Dynamics

We now demonstrate an application of the current code to a realistic accelerator physics problem: the question of emittance growth of the beam due to the resonances in the synchrotron caused by space charge. In all of the test runs done previously the emittance

remained constant during the run. However, if resonances occur, the emittance can grow. To find these resonances, we varied the vertical machine tune ν_{yo} (tune without space charge tune-shift) over a range of 0.85 to 1.3 for three given currents ($I = 0.1$, 0.5, and 1.0 amps).

Each run consisted of 25 turns after which the relative emittance (final emittance divided by initial emittance) was recorded. Figure 3 shows the resulting horizontal and vertical emittances. The dashed line gives the relative emittance for a current of 0.1 amps. For this case there are three resonances with the first two only in the vertical plane. This first is at an integer machine tune of 1.000. This resonance is very narrow, as for a tune of 0.998 or 1.002 there is no emittance growth. The second resonance lies slightly above the integer machine tune. The total tune ($\nu = \nu_o + \Delta\nu$) for this case lies just below 1.0. The third resonance occurs near a machine tune ν_{yo} of 1.13 and a total tune ν_y of 1.12.

The dotted line of Fig. 3 shows the resonances for a current of 0.5 amps. Here again we have the three resonances with only the third having any effect on the horizontal emittance. The first is directly on the integer machine tune, implying that this resonance is tune-shift independent. The second is at a machine tune ν_{yo} of 1.025 and a total tune ν_y of 0.98. The third resonance is at a machine tune ν_{yo} of 1.17 and total tune ν_y of 1.12.

Figure 3's dashed line represents the emittance growth for a current of 1.0 amps. Again we have the same three resonances.

Several things to note about these resonances. The lowest resonance is current independent; it always occurs on the integral machine tune. The second resonance increases in magnitude with current, has a finite width, and only affects the vertical emittance. When total tunes ν_y are used in plotting the data, instead of machine tunes ν_{yo} this second set of resonance points all occur just below 1.0. The third resonance decreases in magnitude with increasing current, and is spread out such that when plotted against total tunes all three occur near a tune of 1.1. The first resonance has a very thin width; however, the other two have distinct widths that increase with current.

6 Conclusion

In this report we have developed a model for tracking a long, ion beam through a synchrotron lattice. We have encoded the equations of motion for the macro-particles into the code SYN2D. Our model has been tested through comparison of its output against theoretical analysis and against the 3-D code SIMPSONS. We have further tested our model by showing that it is able to accurately track the beam at a rate more than twenty times faster than the conventional tracking method. We therefore argue that this new code is preferable to the standard 3-D code. It is more physically justifiable than SIMPSONS for measuring the space charge, as it has a larger concentration of particles per longitudinal unit length and can run with a finer grid. Finally, as it is cheaper to run, it is now possible to track the beam for an entire acceleration cycle (around 100,000 turns). The present tracking algorithm may be further improved by adopting the δf-algorithm as in [13].

We thank Dr. S. Machida for allowing us to use SIMPSONS. Part of the work was supported by Hitachi and DOE.

References

[1] A. Chao, *Physics of Collective Beam Instabilities in High Energy Accelerators*, (John Wiley & Sons, Inc., New York, 1993).

[2] F. Zimmermann, *Proceedings Accelerator Physics at the Superconducting Super Collider*, Dallas, TX, 1992-1993, edited by Y. Yan, *et al.*, p. 98.

[3] N.S. Dikansky and D.V. Pestrikov, *The Physics of Intense Beams and Storage Rings*, (AIP Press, New York, 1994).

[4] R. Baartman, *Proceedings International Workshop on Particle Dynamics in Accelerators: Emittance in Circular Accelerators*, Tsukuba, Japan, 1994, edited by S. Machida and K. Hirata, (KEK, Tsukuba, Japan, 1995), p. 273.

[5] R.C. Davidson, *Physics of Non-Neutral Plasmas*, (Addison-Wesley Publishing, Reading, 1990), Chap. 10.

[6] L. Schachinger and R. Talman, Particle Accelerator **22**, 35 (1987).

[7] S. Machida, *Proceedings Computational Accelerator Physics Conference*, Pleasanton, CA, 1993, edited by R. Ryne, (AIP-297, 1993).

[8] T. Tajima, *Computational Plasma Physics: With Applications to Fusion and Astrophysics* (Addison-Wesley Publishing, Reading, 1989), p. 78.

[9] C. Chen and R.A. Jameson, Phys. Rev. D **52**, 3074 (1995).

[10] S. Machida, "Space Charge Effects in Low Energy Proton Synchrotrons," Ph D. Thesis, University of Tokyo, May 1990.

[11] L.J. Laslett, *Proceedings Summer Study on Storage Rings*, Brookhaven National Laboratory, 1963. (BNL-7534, 1963), p. 324.

[12] E.D. Courant and H.S. Snyder, Ann. Phys. **3**, 1 (1958).

[13] J. K. Koga and T. Tajima, J. Comput. Phys. **116**, 314 (1995).

FIGURE CAPTIONS

FIG. 1. Testing of simulation parameters. (a) Average vertical tune vs. number of macro-particles [N_p = 16 to 4096]. (b) Relative vertical emittance vs. number of macro-particles [N_p = 16 to 4096]. (c) Average vertical tune vs. dimensionless timestep [$d\tau$ = 0.05 to 1.6]. (d) Relative vertical emittance vs. dimensionless timestep [$d\tau$ = 0.05 to 1.6]. [Unless otherwise specified above, the simulation parameters were: Turns= 25, I = 1.0 amps, E = 10 MeV, $\epsilon_x = 50\pi$ mm-mrad, $\epsilon_y = 10\pi$ mm-mrad, $\nu_x = 1.75$, $\nu_y = 0.85$, $d\tau = 0.2$, $N_p = 1024$]

FIG. 2. Comparison of SYN2D with the 3-D code SIMPSONS and theory (a) Horizontal tune-shift vs. current [I = 0.0 to 1.9 amps]. (b) Horizontal tune-shift vs. beam energy [E = 1.0 to 20 MeV]. (c) Horizontal tune-shift vs. horizontal emittance [ϵ_x = 10 to 50π mm-mrad, $\epsilon_y = 10\pi\ mm - mrad$]. (d) Horizontal tune-shift vs. vertical emittance [$\epsilon_x = 10\pi$ mm-mrad, ϵ_y = 10 to 50π mm-mrad].

Solid line is the theoretical tune-shift. Diamonds represent data from our code (SYN2D). Dashes represent data from the 3-D code (SIMPSONS). Error bars denote rms fluctuation in tune-shift over the 25 turns. [Unless otherwise specified above, the simulation parameters were: Turns=25, I = 1.0 amps, E = 10 MeV, $\epsilon_x = 50\pi$ mm-mrad, and $\epsilon_y = 10\pi$ mm-mrad, $\nu_x = 1.75$, $\nu_y = 0.85$, $d\tau = 0.2$, $N_p = 1024$]

FIG. 3. Space charge effect: emittance vs. vertical machine tune. (a) Relative horizontal emittance vs. vertical machine tune. (b) Relative vertical emittance vs. vertical machine tune. Solid line represents I = 0.1 amps. Dashed line represents I = 0.5 amps. Dotted line represents I = 1.0 amps. [Simulation parameters: $I = 0.1, 0.5, 1.0$ amps, E = 10 MeV, $\epsilon_x = 50\pi$ mm-mrad, and $\epsilon_y = 10\pi$ mm-mrad, $\nu_x = 1.75$, $\nu_y = 0.75 \rightarrow 1.30$, $d\tau = 0.2$, $N_p = 1024$]

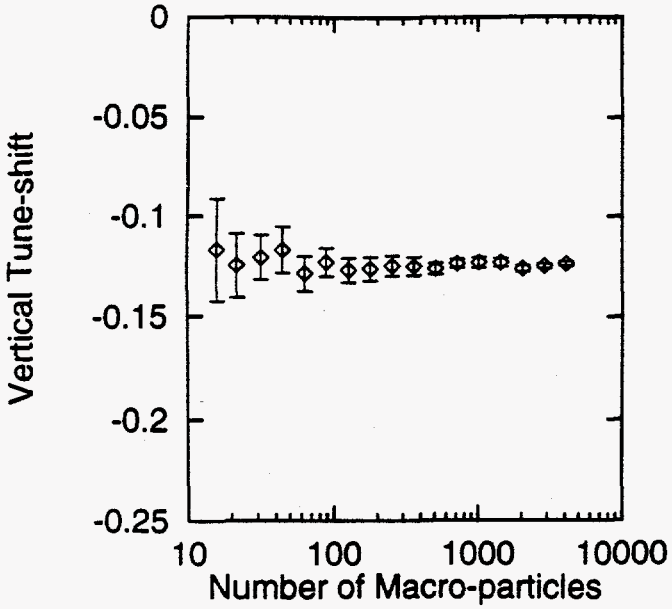
Vertical Tune-shift
0
-0.05
-0.1
-0.15
-0.2
-0.25
10
100
1000
10000
Number of Macro-particles

(a)

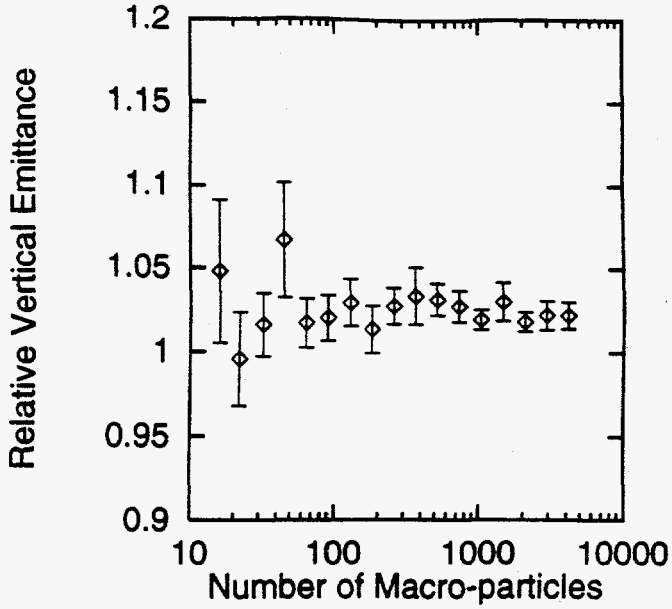
Relative Vertical Emittance
1.2
1.15
1.1
1.05
1
0.95
0.9
10
100
1000
10000
Number of Macro-particles

(b)

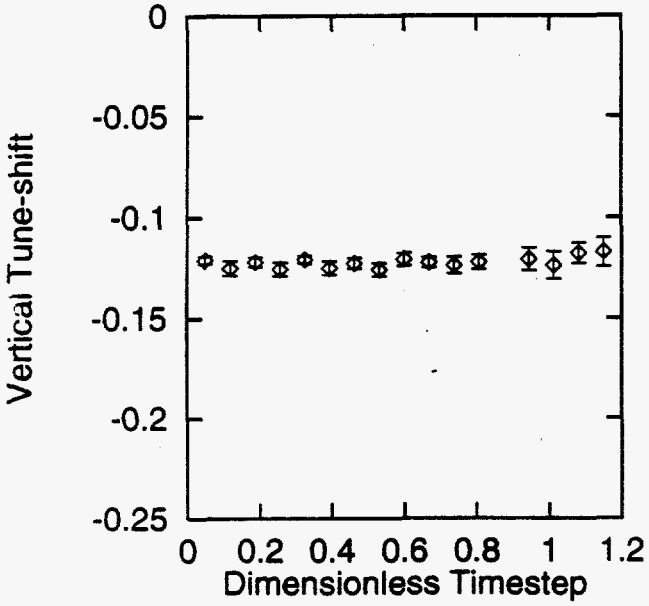
Vertical Tune-shift
0
-0.05
-0.1
-0.15
-0.2
-0.25
0
0.2
0.4
0.6
0.8
1
1.2
Dimensionless Timestep

(c)

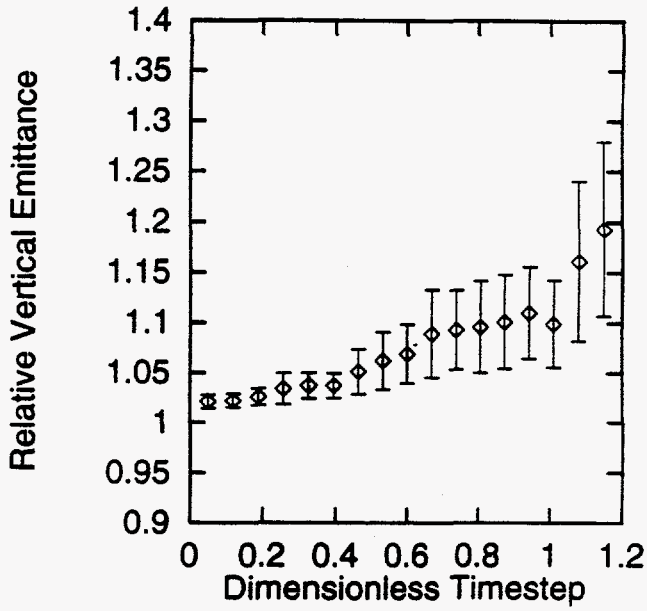
Relative Vertical Emittance
1.4
1.35
1.3
1.25
1.2
1.15
1.1
1.05
1
0.95
0.9
0
0.2
0.4
0.6
0.8
1
1.2
Dimensionless Timestep

(d)

Fig. 1

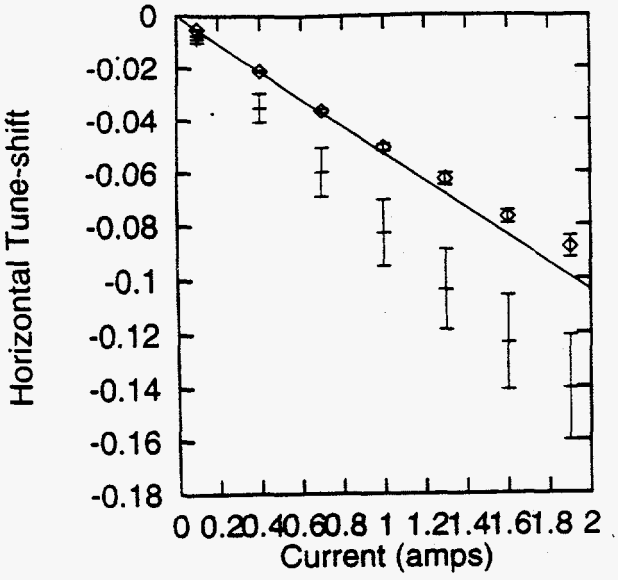
Horizontal Tune-shift
0
-0.02
-0.04
-0.06
-0.08
-0.1
-0.12
-0.14
-0.16
-0.18
0 0.20.40.60.8 1 1.21.41.61.8 2
Current (amps)

(a)

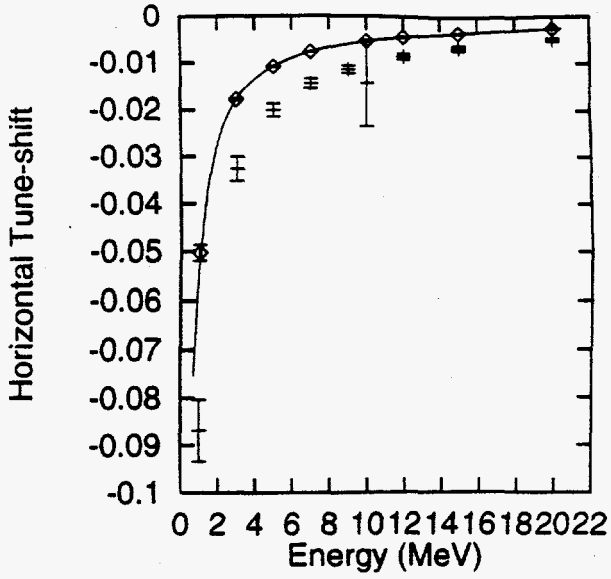
Horizontal Tune-shift
0
-0.01
-0.02
-0.03
-0.04
-0.05
-0.06
-0.07
-0.08
-0.09
-0.1
0 2 4 6 8 10121416182022
Energy (MeV)

(b)

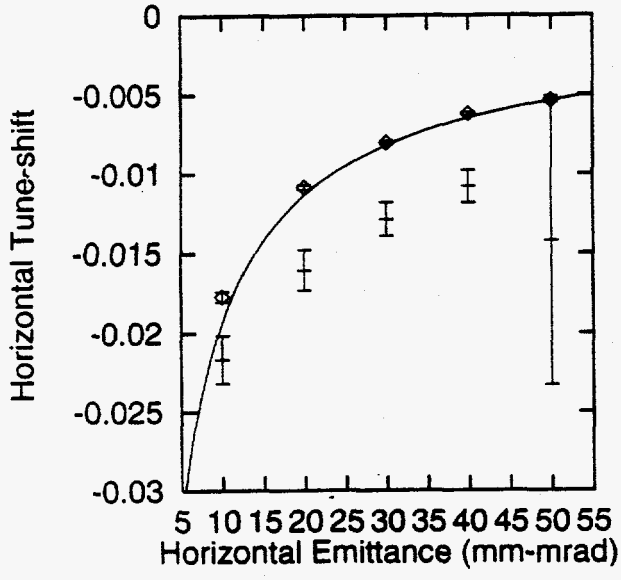
Horizontal Tune-shift
0
-0.005
-0.01
-0.015
-0.02
-0.025
-0.03
5 10 15 20 25 30 35 40 45 50 55
Horizontal Emittance (mm-mrad)

(c)

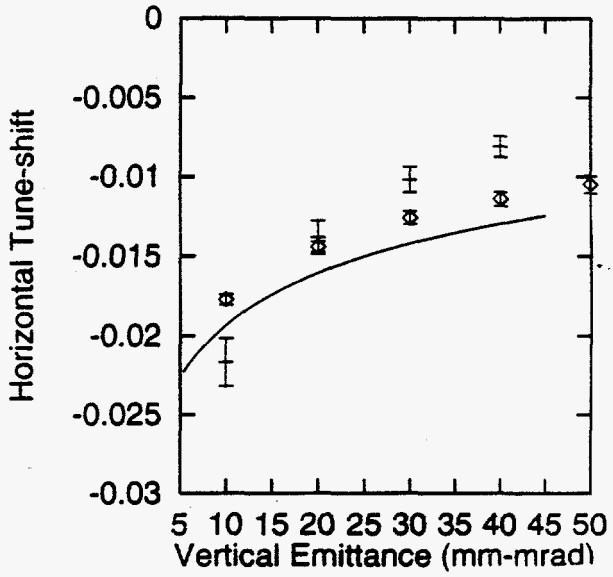
Horizontal Tune-shift
0
-0.005
-0.01
-0.015
-0.02
-0.025
-0.03
5 10 15 20 25 30 35 40 45 50
Vertical Emittance (mm-mrad)

(d)

Fig. 2

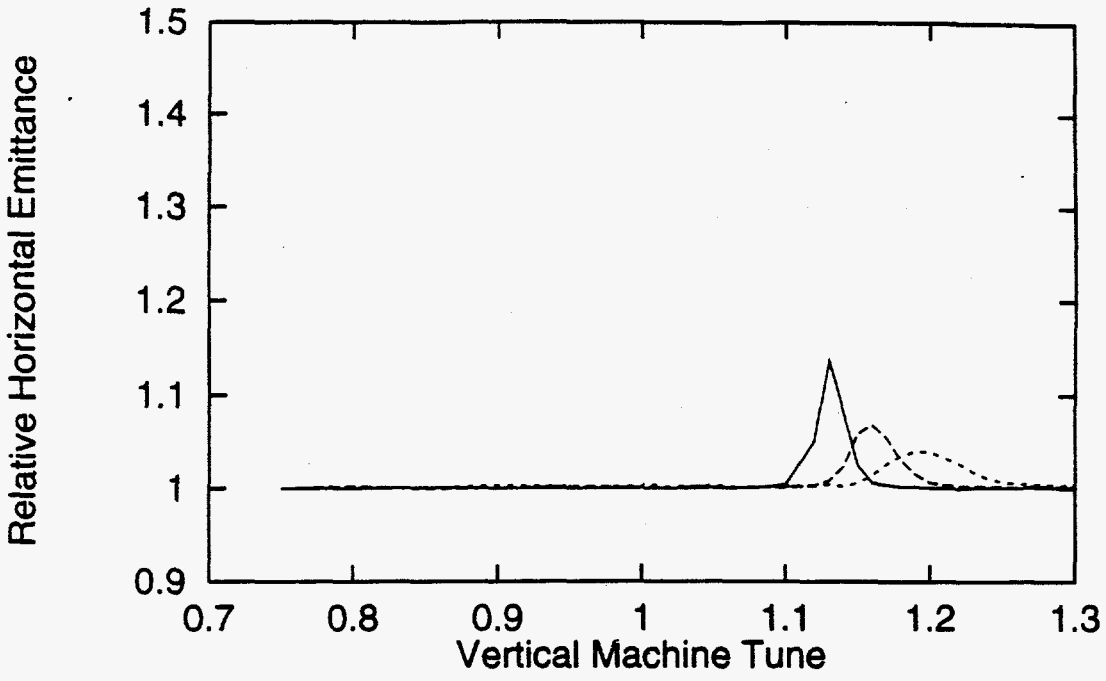
Relative Horizontal Emittance
1.5
1.4
1.3
1.2
1.1
1
0.9
0.7
0.8
0.9
1
1.1
1.2
1.3
Vertical Machine Tune

(a)

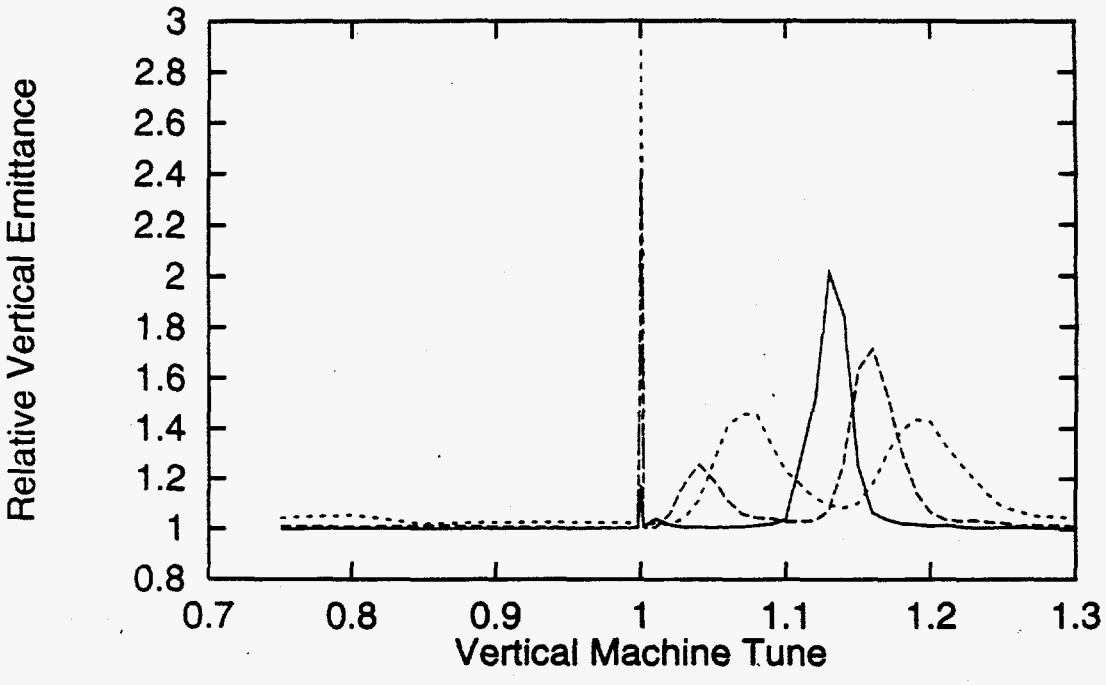
Relative Vertical Emittance
3
2.8
2.6
2.4
2.2
2
1.8
1.6
1.4
1.2
1
0.8
0.7
0.8
0.9
1
1.1
1.2
1.3
Vertical Machine Tune

(b)

Fig. 3